RSC Advances

PAPER

View Article Online
View Journal | View Issue

Cite this: *RSC Adv.*, 2019, **9**, 35841

Heterogeneous photocatalytic performances of CO_2 reduction based on the [Emim]BF_4 + TEOA + H_2O system

Jinliang Lin, * Youfeng Li and Bo Xie

Received 10th August 2019
Accepted 18th October 2019

DOI: 10.1039/c9ra06235a

rsc.li/rsc-advances

The photochemical reduction of CO_2 was studied in a 1-ethyl-3-methylimidazolium tetrafluoroborate, triethanolamine and water ([Emim]BF_4 + TEOA + H_2O) system under visible light irradiation. The integration of CdS and the Co–bpy complex, which acted as a photocatalyst and cocatalyst, respectively, was employed as an efficient catalytic system for the CO_2-to-CO conversion. The utilization of [Emim]BF_4 and water took advantage of their green properties. The amount of CO production showed that the test medium containing 10 vol% H_2O was favourable for the catalytic performance of the CO_2 reduction. In order to further study the factors that influenced the current system, the physical and spectroscopy properties were characterized by altering the composition ratio of the ingredients. Relevant parameters, including the viscosity, conductivity, solubility and coordination, were adjusted using the ratio of the H_2O/[Emim]BF_4 addition, resulting in a different catalytic performance. All of these attempts led to an optimal reaction condition for the CO_2 reduction process.

1 Introduction

In recent decades, the massive consumption of fossil fuels by human beings has caused both energy shortages and excessive CO_2 emission, which have been accompanied by serious environmental changes.[1,2] Meanwhile, CO_2 is also an abundant and sustainable carbon resource that can be used as an industrial feedstock to produce value-added chemicals.[3–5] More specifically, the photocatalytic process addresses the tough challenges and provides a feasible way to use CO_2 as a resource. Therefore, it was simultaneously developed as an approach to store renewable solar energy in the form of chemical energy. In other words, solar energy along with CO_2 can be converted into a high-energy density fuel, which is convenient for transportation and storage. There are a number of works that focus on the photocatalytic CO_2 conversion. To date, these reports are generally classified into following categories: (1) exploiting highly efficient and stable photocatalysts, especially for visible light responding materials;[6,7] (2) the development of reaction types, including the reduction of CO_2 into Cl chemicals and liquid fuels[8] as well as the synthesis of organic compounds such as poly/carbonates, and aromatic carboxylic acids;[9] (3) designing gimmickry or a reaction system for various purposes, especially for green processes and air resistance systems.[10,11] (4) The mechanism investigation is also a promising approach to yield a high efficiency CO_2 conversion.

More specifically, the perspective of green chemistry plays an important role in the design of chemical products and catalytic processes. Water is considered to be a green solvent. Therefore, many CO_2 reduction experiments have been conducted in an aqueous solution over the past few decades. Indeed, the use of water as a reductant and reaction medium provides an ideal approach for the CO_2 conversion with the concept of green chemistry. However, inevitable obstacles exist that hinder the CO_2 reduction reaction. The primary factors include a very low CO_2 solubility (0.033 mol L^{-1} at 25 °C) and hydrogen generation.[12] The poor solubility leads to slow kinetics during the reaction. A competing reaction of the H_2 evolution results in a large consumption of photogenerated electrons.

On the other hand, ionic liquids (ILs) were also reported as green solvents and are widely investigated to address the issues with CO_2 capture and activation.[13] ILs possess many desirable and unique properties for chemical reactions such as wide electrochemical potential window, high ionic conductivity, good thermal and chemical stability as well as low vapour pressure. In particular, they exhibited a high CO_2 solubility.[14] For example, recent research studies proved that an imidazolium-based IL exhibited an excellent performance for the catalytic CO_2 reduction.[15–17] Grills *et al.* revealed that imidazolium cations, a component of IL molecules, can significantly promote the CO_2-to-CO conversion by stabilizing carbonate intermediates.[18] Thus, ILs were widely employed as a reaction medium and catalysts during the electro/chemical reduction of CO_2 in other works.[19–23] However, some inherent drawbacks of ILs hinder their catalytic efficiency such as high viscosity and binding energy. Rosen *et al.* demonstrated the

Department of Chemical and Engineering, Zunyi Normal College, Zunyi, 563000, P. R. China. E-mail: jinliang_lin@163.com; Fax: +86-851-28927159; Tel: +86-851-28927159

production of CO from a CO_2-saturated IL/H_2O solvent with a high faradaic yield and overpotentials below 0.2 V in earlier years.[24] Therefore, to overcome the drawbacks, a study on the CO_2 reduction conducted in an IL/organic or IL/water solution proved ILs to be an outlet in electrochemistry.[25,26] A number of parameters, including the density, viscosity and gas capture behaviour were evaluated in mixtures involving ionic liquids, water and amines.[27] The benefits of the mixture suggested that the strategy of solvent engineering was a feasible way to reduce costs and increase the efficiency towards CO_2 conversion.

With respect to the photocatalytic CO_2 activation, we previously demonstrated a photocatalytic system that exhibited a promotion effect of the ILs for the reduction of CO_2 into CO at 1 atm. In our previous work, the reaction system was tested in a homogenous system and $Ru(bipy)_3Cl_2$ was used as a light photosensitizer.[13] Surely, both ILs and H_2O exhibited potential in the performances for CO_2 reduction. However, the heterogeneous system for the photocatalytic CO_2 conversion in the ILs/H_2O mixture was barely covered. Based on the photocatalytic CO_2 reduction platform that used CdS as a photocatalyst and Co–bpy complex as cocatalyst, the system with volatile organic compounds was expected to be a green and functional solvent. Herein, we reported that the visible light driven catalytic reduction of the CO_2 system was assessed in an ionic liquid medium as well as in the presence of water and triethanolamine (denoted as ([Emim]BF_4 + H_2O + TEOA)) with CdS being employed as a photocatalyst.[13] An innovation in this work was addressing the extension of the green system from a homogenous to heterogeneous process, which allowed for an easier separation and additional recycling. In addition, the relevant physical properties, coordination capability and electrochemical behaviours of the system were evaluated in different conditions. Detailed information on the mechanism of the CO_2 reduction and the design of an environmentally friendly system for the CO_2 reaction was provided.

2 Experimental

2.1 Chemicals

All of the reagents were commercially obtained and used without further purification. 2,2′-Bipyridine (bpy, Alfa), cobalt chloride hexahydrate ($CoCl_2 \cdot 6H_2O$, Sigma), cadmium sulfide (CdS, Sigma, 99.9%) and 1-ethyl-3-methylimidazolium tetrafluoroborate ([Emim]BF_4, ≥98% Shyfhx Co.) were used as received. Triethanolamine (TEOA) was of reagent grade and was purchased from China Sinopharm Chemical Reagent Co. Ltd. The used water was ultrapure with a resistivity of *ca.* 18 mΩ cm^{-1}.

2.2 Viscosity measurement

The viscosity of the reaction medium was measured by an Ubbelohde viscometer (0.47 mm). The testing temperature was maintained at 20 °C. The mixture (10 mL) was prepared in a beaker at different composition ratios by volume (V([EMIM]BF_4) : $V(H_2O)$ = 2 : 8, 4 : 6, 6 : 4 and 8 : 2). Each sample was determined three times in parallel and the average value was taken.

2.3 Spectrographic characterization

Absorption spectra were obtained on a UV-Vis spectrophotometer (Varian Cary 500). The samples were prepared in 5 mL solvents ([Emim]BF_4, H_2O or TEOA) with different solutes ($CoCl_2$ or $Co(bpy)_3Cl_2$). To determine the $Co(bpy)^+$ transition, the experiment was conducted in a sealed container adaptable for the recording equipment and the compound was exposed to light irradiation for 30 min before the test.

2.4 Conductivity test

The electrical conductivity was measured on a conductivity meter (DDSJ-318, INESA Scientific Instrument Co. Ltd). The mixture (10 mL) was added in the electrolysis cell at different composition ratios by volume, which was the same as the viscosity measurement. The electrolysis cell was placed in a constant temperature water bath at 20 °C. Each sample was analyzed three times in parallel and the average value was taken.

2.5 Photocatalysis activity test

All of the experiments were performed in a Schlenk flask (80 mL) under an atmosphere of CO_2. In the Schlenk flask, CdS (50 mg) and $CoCl_2 \cdot 6H_2O$ (10 μmol) were added to a 5 mL mixture of (solvent + water)/TEOA (4 : 1 by volume). This mixture system was subjected to vacuum degassing and backfilling with pure CO_2 gas. This process was repeated (3 times) and after the last cycle, the flask was back-filled with CO_2. Then, the system was irradiated for 2 hours with four 300 W LED light sources under vigorous stirring at 20 °C with a controlled water-cooling system. The produced gases (CO and H_2) were detected using a gas chromatography system (Agilent 7890B, Agilent Technologies) equipped with a packed molecular sieve column (TDX-1 mesh 42/10). Ar was used as the carrier gas for the GC.

3 Results and discussion

The photocatalytic performance was tested by fixing the total volume at 5 mL and the volume of TEOA at 1 mL, while altering the addition of H_2O and [Emim]BF_4. As illustrated in Fig. 1, the amount of gaseous production (CO and H_2) was closely related to the ratio of [Emim]BF_4/water in the reaction medium. Under anhydrous conditions, the evolution of CO and H_2 was moderate (11.2 and 5.6 μmol) under visible light illumination. An increasing evolution of CO was observed after adjusting the H_2O content from 0 mL to 10 vol%. 31.8 μmol of CO was obtained in the reaction medium containing 10% H_2O by volume. Clearly, the reaction was more feasible to start with H_2O, as both electrons and holes preferred charged reaction partners. Afterwards, the addition of H_2O resulted in decrements towards the production of CO. The activity for the CO production (3.1 μmol) was also sluggish when [Emim]BF_4 was removed, which was lower than that without H_2O (11.0 μmol). However, a gradually increased yield of H_2 was generated when the system increased

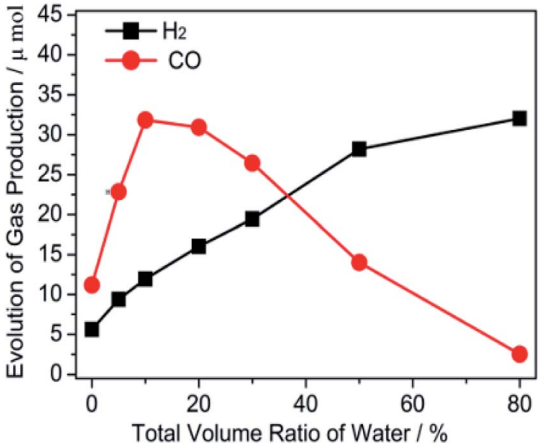

Fig. 1 The effect of the different volume ratios of the [Emim]BF_4/H_2O/TEOA medium on the gas evolution of CO and H_2.

the amount of H_2O. Obviously, the production of both CO and H_2 were closely related to the different ratios of [Emim]BF_4/H_2O. The result suggested that there was a synergistic effect for [Emim]BF_4 and H_2O, which played a vital role in the enhancement of the photocatalytic performance of the CO_2 reduction. It is well known that [Emim]BF_4 possesses a high viscosity, which affects the mass transfer. We can acknowledge from the above result that the role of water in the adjustment of the catalytic performance was related to the dilution effect and proton source supplier.

The hypothesis for the relationship between the catalytic performance and viscosity was still unclear when H_2O was used as a conditioning agent because H_2O also acted as a hydrogen source that affected the catalytic performance. It is well known that the viscosity can be easily adjusted by temperature. Thus, a further reaction was conducted at a different temperature. It should be mentioned that the influence of the molecular activation by the finite-amplitude temperature was negligible in this study. Based on above results, we fixed a 10 vol% H_2O solution as the reaction medium for this study. As shown in Fig. 2, a low catalytic performance for both, the H_2 and CO evolution, was obtained at 5 °C, which was attributed to the viscous solution impeding the mass transfer. Generally, a steadily increasing evolution rate for H_2 was obtained as the temperature increased. An increasing amount of CO was generated when the temperature rose from 5 °C to 20 °C. This meant that the mobility of the reaction medium promoted both the CO_2 and H_2O reduction. Afterwards, the increase in the temperature resulted in a negative effect on CO evolution. A gradual decrease in the CO selectivity was therefore exhibited in this figure when the temperature was increased. This phenomenon was mainly caused by the high temperature leading to a low CO_2 solubility. The formation of the CO_2^- intermediate transition was an adverse process when CO_2 escaped from the solution.

As shown in Fig. 3, the viscosity of the [Emim]BF_4/H_2O/TEOA solution continuously decreased with the increase in the H_2O volume fractions. Meanwhile, the conductivity of the [Emim]BF_4/H_2O/TEOA solution increased as the H_2O volume fractions increased in the low concentration range. After reaching a maximum value of 32.5 mS cm^{-1} at 50 vol%, the conductivity of the solution started to decrease with an increasing H_2O concentration. At the initial stage, the change in the conductivity was consistent with the catalytic performance when the water content was within 10 vol%. The viscosity of the solution was 7.8 mPa s. The reaction medium with a low concentration of water provided a proper viscosity and proton supply. The lower viscosity resulted in a high efficiency by accelerating the mass transfer, which was evidently reflected by increasing the conductivity. Another reason to boost the CO evolution originated from the water addition, providing a typical hydrogen source for the dispersed surrounding CO_2 molecules, which were readily available for the proton coupling process. Both promoted the photocatalytic CO_2 reduction. However, the maximum conductivity for the water content at 50 vol% was different from that of the catalytic performance at 10 vol%. The decreasing CO evolution suggested a mass-transfer and

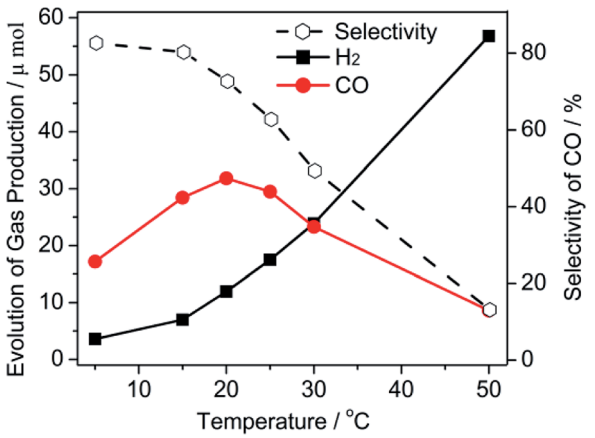

Fig. 2 The gas evolution of CO and H_2 and the selectivity of CO as a function of the temperature (selectivity of CO = mol CO/mol (H_2 + CO) × 100).

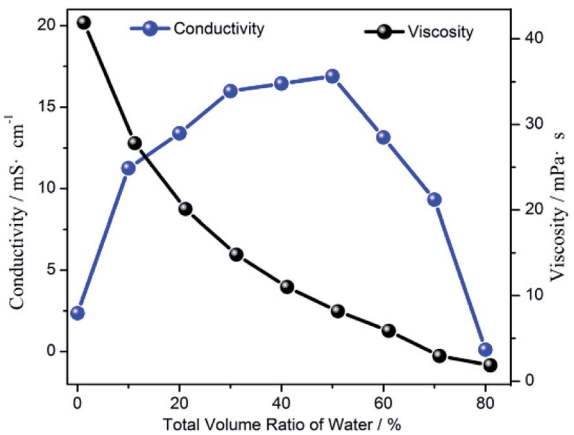

Fig. 3 The viscosity and the electrical conductivity of the [Emim]BF_4/H_2O solution as a function of the water volume fraction.

solubility process that had a negative effect on CO_2 transfer, while promoting the competitive reaction of hydrogen (H_2) evolution.

The spectrochemical method revealed a definite catalytic mechanism that may provide important insights for the further rational design of the catalytic system. Thus, a UV-Vis absorption measurement was conducted to collect the coordination information for the selected solvents. Initially, in order to evaluate the coordination capabilities of the metal center with solvent molecules, the experiments were tested in solutions by directly dissolving Co^{2+} ($CoCl_2$) in an aqueous solution and [Emim]BF_4, respectively.[28] The UV-Vis absorption spectra (Fig. 4) obtained in both solutions generally exhibited two absorption bands. The absorption bands located within the ultraviolet region were attributed to the ligand π–π* transition and a red-shift likely from a metal-to-ligand charge transition (MLCT) band (Fig. 4A and B, black line).[29] The absorption bands positioned in the visible region were due to the d–d transition (Fig. 4A and B, black line).[30] A different absorption region was also presented in the spectra of an aqueous solution (410–570 nm, Fig. 4A, red line) and [Emim]BF_4 solution (500–715 nm, Fig. 4B, red line). This observation indicated a different interaction between the ligand part and metal center in the current system when water and [Emim]BF_4 were used as the reaction medium.

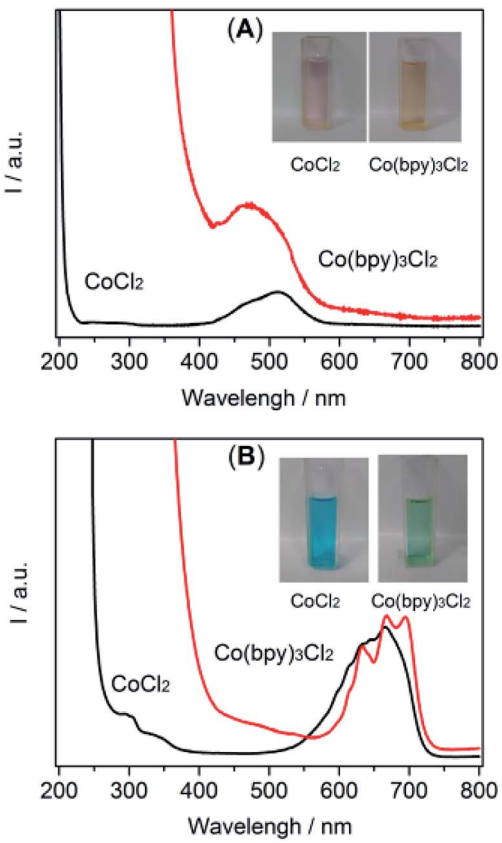

Fig. 4 UV-Visible absorption spectra of $CoCl_2$/$Co(bpy)_3Cl_2$ recorded in water (A) and [Emim]BF_4 (B) solutions. (Inset shows the corresponding photograph of each sample).

Fig. 4B displays the UV-Vis absorption spectra of the solution in the presence of bpy. As shown, after the introduction of bpy, the absorption position extending to the near-ultraviolet region experienced an obvious red-shift, highlighting the enhanced MLCT process. A new absorption (peaks at 450 nm) appeared in the $CoCl_2$/bpy containing aqueous solution, while the absorption intensity at 410–570 nm was weakened. This change made the solution turn from red to an orange colour. In the [Emim]BF_4 solution, a red-shift near 400 nm and an alternation in 550–725 nm appeared, which resulted in a colour change from blue to green. Compared with the solution without bpy, these results indicated that the cobalt center was favored to coordinate with bpy and form $Co(bpy)_3Cl_2$ in these two solvents. It also should be noted that there were different absorptions between the solutions of [Emim]BF_4 and H_2O. These changes were mainly induced by the alternation in the chemical nature of the solvent molecules such as the charge transfers between the solvent and metal ions, solvent dependent aggregation and complexation.[31] In addition, the tertiary amine, TEOA, may have also contributed to the solvent effect in the photocatalytic CO_2 reduction systems by surviving as a ligand to coordinate with the cobalt center. The results of the UV-Vis absorption characterizations demonstrated that the ligand (*e.g.*, bpy) in the CO_2 reduction system altered the charge distribution of the metal center and eventually affected the CO_2 adsorption and the catalytic performance of the CO_2 reduction system. In addition, the spectra also presented solid evidence of a coordination effect between the cobalt center and [Emim]BF_4 or H_2O.

Interestingly, before the photocatalytic reaction, all of the coordination sites for cobalt were occupied by three bipyridine molecules (six N atoms) and should not have been affected by the local environments. Therefore, a confirmation in the vacancy of the Co complex was further investigated. As demonstrated in Fig. 5, a new absorption range from 500–750 nm was observed during light irradiation, which suggested that $Co(bpy)^+$ was formed.[32] The orange suspension turned dark blue during irradiation. The color shift was probably related to

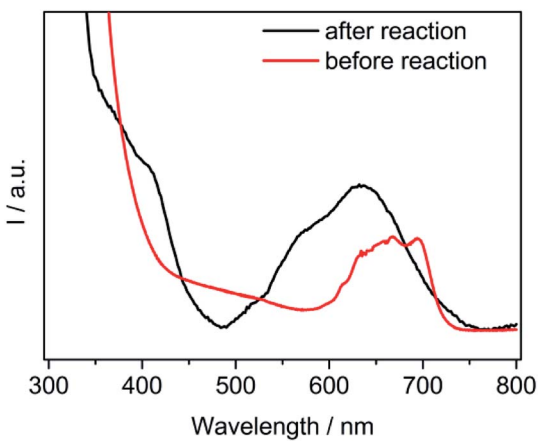

Fig. 5 Absorption spectra of the $Co(bpy)^{2+}$ complexes (before reaction) and $Co(bpy)^+$ complexes (after reaction). The ingredients in the solution were the same as the reaction with 10 vol% H_2O.

Co(I) πd to bpy π* back-bonding in the $Co(bpy)_n^+$ series. In addition, the occurrence of a partial dissociation between cobalt and bpy generated the possibility of anchoring again with the surrounding solvent molecules. This spectroscopic result provided evidence in support of the speculates that coordinated between the $Co(bpy)^+$ complexes and solvents.

In fact, the redox process for the Co-complex was previously inspected by electrochemical experiments.[33] Those reports indicated an existence of $Co^{II/I}$ and $Co^{I/0}$ redox pairs during cyclic voltammetry (CV) scans. The generation of Co(I) species subsequently served as an important activated catalyst for CO_2. Further observations verified the binding of CO_2 with the Co(I) species to give a $[Co–CO_2]^-$ adduct. It is well known that the electrochemical behaviors are strongly influenced by surrounding factors. Ionic liquids such as $[Emim]BF_4$ can greatly lower the over-potentials of the CO_2 reduction.[24] It happened that there was a similar case. The electrocatalysts were able to facilitate the proton-coupled multi-electron reactions, which required lower potentials than that for the single-electron reaction occurring at −1.9 V. These results indicated that the ingredients water and $[Emim]BF_4$ in a proper proportion simultaneously exhibited a synergistic effect for the catalytic CO_2 reduction.

Hence, the mechanism for the catalytic CO_2 reduction by a $CdS/Co(bpy)_3^{2+}$ hybrid catalytic system was described in previous reports.[34] CdS liberated the electrons upon light irradiation. The Co(II) complex with bipyridinium, an electron-withdrawing anchoring group, easily grasped the electrons and then turned into an active Co(I) intermediate.[35] At this stage, one of the functions of water was that of a diluting agent, which lowered the viscosity of the reaction medium. It promoted the mass transfer process by enhancing the mobility, which was directly recorded by the high conductivity (Fig. 2).

Next, as confirmed in Fig. 5, one bipyrimidine ligand left the metal center. Therefore, the molecular compounds ($[Emim]^+$, H_2O, TEOA) around the complex may have come into contact with the metal centers and functioned as a stabilizer for a highly unstable intermediate (Fig. 4). A reasonable example in a cobaltic system was reported that involved an ionic liquid with an imidazole-group function, serving as a stabilizer of the Co^I species.[36] The reductive cobalt intermediate allowed for a strong interaction with CO_2 to form a metal carbonate. It should be noted that $[Emim]BF_4$ with a high CO_2 solubility assisted the combination rate for CO_2 and cobalt. On the other hand, many proton sources dissociated from water. Therefore, the protonation promoted the cleavage of the C–O bond in the $[Co–CO_2]^-$ adduct and resulted in the yield of CO.[37] The H_2 evolution with a combination of a Co(I) intermediate with protons to form the Co(III)-hydride was probably similar to the CO_2 conversion.[38] During the catalytic processes, the generation and stability of the active species was greatly enhanced by the favorable chemical environments of the reaction medium.[39] More specifically, the coordination ability of $[Emim]BF_4$ contributed to this process, and thereafter promoted the final CO_2 conversion. As expected, the process for the charge transfer between the cobalt ion and coordinated CO_2 was inevitably influenced by the nature of $[Emim]BF_4$.

4 Conclusions

In summary, a heterocatalytic system was mediated by $[Emim]BF_4/H_2O$/TEOA for the selective reduction of CO_2. The influence factors for the catalytic performance were characterized in detail. (i) The role of water was that of a dilution agent to adjust the viscosity of the current system and that of a proton source to assist the proton-coupling process, which was responsible for the CO_2 conversion. (ii) The activity and selectivity were closely related to the viscosity and conductivity. (iii) The coordination between the metal center and $[Emim]^+$ may have promoted the stability of the CO_2 intermediates. Therefore, all of these results were helpful for studying a broader range of the green system, developing a new, efficient, artificial photosynthesis system, better understanding composition–activity relationships and optimizing this system.

Conflicts of interest

There are no conflicts to declare.

Acknowledgements

This work was sponsored by the Natural Science Foundation of Guizhou Province Education Department ([2018]311) and the Natural Science Foundation of Guizhou Province ([2016]7011 & [2017]5727-11).

Notes and references

1 M. He, Y. Sun and B. Han, *Angew. Chem., Int. Ed.*, 2013, **52**, 9620–9633.
2 I. Yasuo, *Coord. Chem. Rev.*, 2013, **257**, 171–186.
3 W. L. Dai, L. Chen, S. F. Yin, W. H. Li, Y. Y. Zhang, S. L. Luo and C. T. Au, *Catal. Lett.*, 2010, **137**, 74–80.
4 X. Shi, Z. Q. Han, X. L. Peng, P. Richard, T. Qian, X. X. Wu, M. W. Qiu, S. C. Wang, J. P. Hu, Y. J. Sun and H. Ding, *Nat. Chem.*, 2017, **9**, 1019.
5 L. Q. He, H. Yang, J. J. Huang, X. H. Lu, G. R. Li, X. Q. Liu, P. P. Fang and Y. X. Tong, *RSC Adv.*, 2019, **9**, 10168–10173.
6 J. L. Lin, Z. M. Pan and X. C. Wang, *ACS Sustainable Chem. Eng.*, 2013, **2**(3), 353–358.
7 L. Yuan and Y. J. Xu, *Appl. Surf. Sci.*, 2015, **342**, 154–167.
8 J. Wei, Q. Ge, R. Yao, Z. Wen, C. Fang, L. Guo, H. Xu and J. Sun, *Nat. Commun.*, 2017, **8**, 15174.
9 H. Kawanami, A. Sasaki, K. Matsui and Y. Ikushima, *Chem. Commun.*, 2003, **34**(31), 896–897.
10 C. Guan, Y. P. Pan, E. P. L. Ang, J. S. Hu, C. G. Yao, M. H. Huang, H. F. Li, Z. P. Lai and K. W. Huang, *Green Chem.*, 2018, **20**, 4201–4205.
11 R. Snoeckx and A. Bogaerts, *Chem. Soc. Rev.*, 2017, **46**, 5805–5863.
12 M. Jitaru, *J. Univ. Chem. Technol. Metall.*, 2007, **42**(4), 333–344.
13 J. L. Lin, Z. X. Ding, Y. D. Hou and X. C. Wang, *Sci. Rep.*, 2013, **3**, 1056.

14 S. Bazhenov, M. Ramdin, A. Volkov, V. Volkov, T. J. H. Vlugt and T. W. D. Loos, *J. Chem. Eng. Data*, 2014, **59**(3), 702–708.
15 J. P. Feng, S. J. Zeng, J. Q. Feng, H. F. Dong and X. P. Zhang, *Chin. J. Chem.*, 2018, **36**(10), 961–970.
16 J. P. Feng, S. J. Zeng, H. Z. Liu, J. Q. Feng, H. S. Gao, L. Bai, H. F. Dong, S. J. Zhang and X. P. Zhang, *ChemSusChem*, 2018, **11**(18), 3191–3197.
17 Y. L. Gu, Q. H. Zhang, Z. Y. Duan, J. Zhang, S. G. Zhang and Y. Q. Deng, *J. Org. Chem.*, 2005, **70**(18), 7376–7380.
18 D. C. Grills, Y. Matsubara, Y. Kuwahara, S. R. Golisz, D. A. Kurtz and B. A. Mello, *J. Phys. Chem. Lett.*, 2014, **5**, 2033–2038.
19 Y. Oh and X. L. Hu, *Chem. Soc. Rev.*, 2013, **42**, 2253–2261.
20 B. C. M. Martindale and R. G. Compton, *Chem. Commun.*, 2012, **48**, 6487–6489.
21 D. Zhao, M. Wu, Y. Kou and E. Min, *Catal. Today*, 2002, **74**, 157–189.
22 M. Galinski, A. Lewandowski and I. Stepniak, *Electrochim. Acta*, 2006, **51**, 5567–5580.
23 S. M. Xia, K. L. Chen, C. H. Fu and L. N. He, *Front. Chem.*, 2018, **6**, 468.
24 B. A. Rosen, A. S. Khojin, M. R. Thorson, W. Zhu, D. T. Whipple, P. A. Kenis and R. I. Masel, *Science*, 2011, **334**(6056), 643–644.
25 D. W. Yang, Q. Y. Li, F. X. Shen, Q. Wang, L. Li, N. Song, Y. N. Dai and J. Shi, *Electrochim. Acta*, 2016, **189**, 32–37.
26 T. N. Huan, P. Simon, G. Rousse, I. Génois and V. A. M. Fontecave, *Chem. Sci.*, 2017, **8**(1), 742–747.
27 Y. S. Zhao, X. P. Zhang, S. J. Zeng, Q. Zhou, H. F. Dong, X. Tian and S. J. Zhang, *J. Chem. Eng. Data*, 2010, **55**(9), 3513–3519.
28 P. F. Zhang, Y. T. Gong, Y. Q. Lv, Y. Guo, Y. Wang, C. M. Wang and H. R. Li, *Chem. Commun.*, 2012, **48**, 2334–2336.
29 T. Shimoda, T. Morishima, K. Kodama, T. Hirose, D. E. Polyansky, G. F. Manbeck, J. T. Muckerman and E. Fujita, *Inorg. Chem.*, 2018, **57**, 5486–5498.
30 K. Sivaraj and K. P. Elango, *J. Solution Chem.*, 2010, **39**, 1681–1697.
31 G. Goutam and G. Suhrit, *Chem. Commun.*, 2018, **54**, 5720–5723.
32 H. A. Schwarz, C. Creutz and N. Sutin, *Inorg. Chem.*, 1985, **24**(3), 433–439.
33 N. V. Rees and R. G. Compton, *Energy Environ. Sci.*, 2011, **4**, 403–408.
34 Z. G. Chai, Q. Li and D. S. Xu, *RSC Adv.*, 2014, **4**, 44991–44995.
35 M. Cheng, X. Yang, J. Li, C. Chen, J. Zhao, Y. Wang and L. Sun, *Chem.–Eur. J.*, 2012, **18**(50), 16196–16202.
36 Y. Hori, B. H. Wake, T. Tsukamoto and O. Koga, *Electrochim. Acta*, 1994, **39**, 1833–1839.
37 Y. A. Daza and J. N. Kuhn, *RSC Adv.*, 2016, **6**(55), 49675–49691.
38 S. C. Marinescu, J. R. Winkler and H. B. Gray, *Proc. Natl. Acad. Sci. U. S. A.*, 2012, **109**, 15127–15131.
39 J. L. Lin, B. Qin and G. L. Zhao, *J. Photochem. Photobiol., A*, 2018, **354**, 181–186.